Available online at www.sciencedirect.com
ScienceDirect
European Polymer Journal 43 (2007) 3522–3530
EUROPEAN POLYMER JOURNAL
www.elsevier.com/locate/europolj

Amphiphilic biodegradable poly(CL-*b*-PEG-*b*-CL) triblock copolymers prepared by novel rare earth complex: Synthesis and crystallization properties

Weipu Zhu, Weihui Xie, Xiaowei Tong, Zhiquan Shen *

Institute of Polymer Science, Zhejiang University, Key Laboratory of Macromolecule Synthesis and Functionalization of Ministry of Education, Hangzhou, Zhejiang 310027, China

Received 18 January 2007; received in revised form 5 April 2007; accepted 19 April 2007
Available online 3 May 2007

Abstract

Amphiphilic biodegradable poly(CL-*b*-PEG-*b*-CL) triblock copolymers have been successfully prepared by the ring-opening polymerization of ε-caprolactone (CL) employing yttrium tris(2,6-di-tert-butyl-4-methylphenolate) [$Y(DBMP)_3$] as catalyst and double-hydroxyl capped PEGs (DHPEG) as macro-initiator. The triblock architecture, molecular weight, thermal and crystallization properties of the copolymers were characterized by NMR spectra, SEC, DSC and WAXD analyses. The isothermal crystallization behavior of the copolymers was investigated by POM analysis in detail, which is greatly influenced by the length of PCL and PEG blocks. On the POM micrograph of $PEG_{10,000}$–$(PCL_{8600})_2$, a unique morphology of concentric spherulites was observed due to the sequent crystallization of the PCL and PEG blocks.

Keywords: Block copolymer; Isothermal crystallization; Poly(ε-caprolactone); Poly(ethylene glycol); Rare earth catalyst

1. Introduction

Amphiphilic block copolymers with hydrophilic and hydrophobic blocks have attracted much attention in recent years [1,2]. The hydrophobic blocks in an aqueous phase undergo macromolecular assembly to generate polymeric micelles and micelle-like aggregates. The novel characteristics of polymeric micelles such as thermodynamic stability and the nanosized core-shell structure have found many applications in the field of drug delivery [3,4] and separation technology [5].

Poly(ε-caprolactone) (PCL) is one of the most attractive and promising biodegradable aliphatic polyesters due to its good drug permeability, biocompatibility and non-toxicity [6]. Poly(ethylene glycol) (PEG) is a highly hydrophilic and biocompatible poly(ether), which has been widely used to form various amphiphilic block copolymers with hydrophobic segments such as poly(ester), poly(carbonate), and poly(amino acid) [7,8]. Recently, PEG–PCL block copolymers have been prepared by the ring-opening polymerization of ε-caprolactone (CL) using

* Corresponding author. Fax: +86 571 87953727.
E-mail addresses: carrols@163.com (W. Zhu), weihui831026@163.com (W. Xie), tongxiaowei@zju.edu.cn (X. Tong), zhiquan_shen@163.com (Z. Shen).

0014-3057/$ - see front matter © 2007 Elsevier Ltd. All rights reserved.
doi:10.1016/j.eurpolymj.2007.04.024

PEG as macro-initiators with stannous octanoate [$Sn(Oct)_2$] as catalyst [9]. Furthermore, a few new catalysts such as zinc [10], calcium [11] and aluminum [12] complexes were developed for the synthesis of amphiphilic copolymers containing PEG blocks.

Both drug permeability and biodegradability rely on the crystallinity of the polymer. However, the studies on the morphology and the crystallization (melting) properties of such copolymers are rather limited and not systematic. According to Gan's work [13] on PEG–PCL diblock copolymers, the PCL block is crystallizable while the PEG content is lower than 20 wt.%. Chen's studies [14,15] on PEG–PCL diblock copolymers suggested that if the PCL block was longer than the PEG block, the PCL block crystallized first and fixed the total structure of the spherulites, when cooling from a molten state and led to obviously imperfect crystallization of PEG. The PEG block could still crystallize at −6.6 °C even when its fraction is only 14 wt.%.

In our continuing studies on the controlled ring-opening polymerization of lactones, lactides and cyclic carbonates, a series of rare earth phenolate complexes have been found to be efficient catalysts for CL homo- and co-polymerization with high activity, good controllability and low toxicity [16–19]. In this work, yttrium tris(2,6-di-tert-butyl-4-methylphenolate) [$Y(DBMP)_3$] has been firstly employed for poly(CL-*b*-PEG-*b*-CL) synthesis with a series of double-hydroxyl capped PEGs (DHPEG) as macro-initiators under mild conditions. The thermal and crystallization properties of the copolymers were investigated by DSC, WAXD and POM analyses in detail.

2. Experimental

2.1. Material

$Y(DBMP)_3$ and pure $PCL_{30,000}$ homo-polymer were synthesized as we reported formerly [16,17]. ε-Caprolactone (Acros) was distilled under reduced pressure prior to use. DHPEGs (Shanghai Chemical Co.) were dried by an azeotropic distillation with dry toluene before use. Other reagents and solvents were purified by general methods.

2.2. Polymerization

All polymerizations were carried out in previously flamed 15 ml ampoules under dry argon with Schlenk techniques. A mixture of DHPEG and $Y(DBMP)_3$ were dissolved in THF with certain molar ratio and kept in a water bath at 40 °C for 15 min aging before the CL monomer was injected into the ampoule by a syringe. After the desired polymerization time, the polymerization was quenched by ethanol containing 5% hydrochloric acid (HCl), the mixture was poured into a large excess of ethanol, and the polymer precipitated from ethanol, filtered and dried in vacuum to constant weight.

2.3. Measurements

Nuclear magnetic resonance (NMR) spectra were recorded on a Bruker Avance DMX500 spectrometer in $CDCl_3$ with tetramethylsilane as internal standard. Size-exclusion chromatographic (SEC) measurements calibrated to commercial polystyrene standards were performed on a Waters 150-C apparatus with columns Styragel HT 3, HT 4, HT 5 and Waters 2410 RI detector in THF (1.0 ml/min) at 25 °C. Differential scanning calorimetry (DSC) measurements were performed on a TA Q100 apparatus. The samples were heated to 100 °C, held for 2 min to erase the thermal history, then cooled to −30 °C at a rate of 10 °C /min, and finally heated to 100 °C at 10 °C/min rate again. The crystal structures of triblock copolymers were examined by wide-angle X-ray diffraction (WAXD) at a Rigaku D/max-rA X-ray diffractometer with Cu Kα radiation of wavelength $\lambda = 1.54056$ Å for 2θ angles between 5° and 50° at a scanning speed of 2.0°/min. The samples used for polarized optical microscope (POM) measurement were prepared by casting three drops of a 1.0 wt.% chloroform solution of the copolymers on a clean cover glass and then airing for 24 h at room temperature followed by drying under vacuum for 24 h. The morphologies of poly(CL-*b*-PEG-*b*-CL) triblock copolymers were monitored with an Olympus BX51 POM equipped with crossed polarizer.

3. Results and discussion

3.1. Synthesis and characterization

DHPEGs with molecular weights of 200, 1000, 2000, 4000 and 10,000 were used. $Y(DBMP)_3$ containing the Y-OAr bond reacts with hydroxyl end groups of DHPEG, forming alkoxide containing a Y–OR bond that can initiate the polymerization

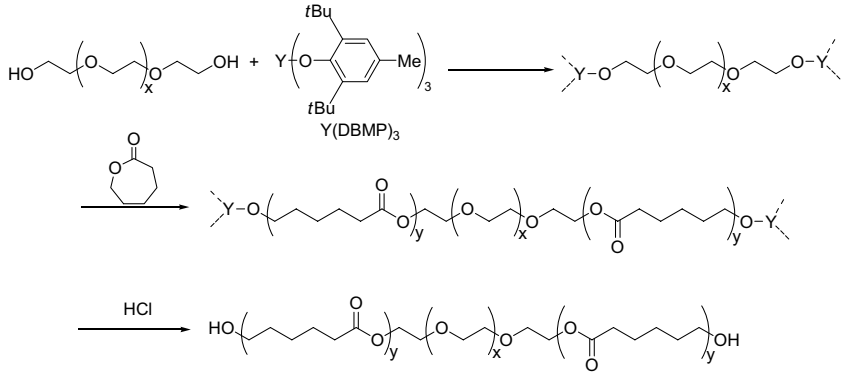

Scheme 1. Synthesis of poly(CL-*b*-PEG-*b*-CL) catalyzed by $Y(DBMP)_3$.

Table 1
Poly(CL-*b*-PEG-*b*-CL) triblock copolymers prepared by DHPEGs and $Y(DBMP)_3$[a]

Polymer	$\frac{[CL]}{[DHPEG]}$	$\frac{[DHPEG]}{[Y(DBMP)_3]}$	Conv. (%)	$[\eta]$ (dl/g)	[b] $M_{n,}^{cal}$ (Kg/mol)	[c] $M_{n,}^{NMR}$ (Kg/mol)	[d] $M_{n,}^{SEC}$ (Kg/mol)	[d] MWD
PEG_{200}–$(PCL_{2300})_2$	40	4	>99	0.12	4.8	3.7		
PEG_{200}–$(PCL_{4000})_2$	70	4	>99	0.16	8.2			
PEG_{200}–$(PCL_{7100})_2$	125	4	>99	0.27	14.4			
PEG_{200}–$(PCL_{14,300})_2$	250	2	>99	0.30	28.7	30.1		
PEG_{1000}–$(PCL_{2000})_2$	35	4	>99	0.11	5.0			
PEG_{1000}–$(PCL_{4000})_2$	70	4	>99	0.13	9.0			
PEG_{1000}–$(PCL_{8400})_2$	150	2	98.2	0.29	19.1	17.4		
PEG_{1000}–$(PCL_{13,800})_2$	250	2	97.3	0.35	28.7	30.4		
PEG_{2000}–$(PCL_{1800})_2$	35	2.5	90.9	0.11	5.6			
PEG_{2000}–$(PCL_{3600})_2$	70	2.5	89.3	0.15	9.1			
PEG_{2000}–$(PCL_{8300})_2$	150	2	97.5	0.26	18.6	18.3	17.0	1.3_7
PEG_{2000}–$(PCL_{14,300})_2$	250	2	>99	0.36	30.4	29.8	19.8	1.5_6
PEG_{4000}–$(PCL_{2300})_2$	40	2.5	>99	0.12	8.3			
PEG_{4000}–$(PCL_{3200})_2$	60	2.5	92.6	0.17	10.1	10.2	7.4	1.3_9
PEG_{4000}–$(PCL_{8400})_2$	150	2	98.5	0.28	20.8	21.3	14.3	1.4_5
PEG_{4000}–$(PCL_{13,600})_2$	250	2	95.7	0.35	31.3	32.1	19.3	1.5_8
$PEG_{10,000}$–$(PCL_{3300})_2$	70	1.5	82.6	0.22	16.6	17.1	11.5	1.2_9
$PEG_{10,000}$–$(PCL_{8600})_2$	150	1.5	>99	0.28	27.1	28.2	15.1	1.3_5
$PEG_{10,000}$–$(PCL_{14,300})_2$	250	1.5	>99	0.40	38.5	40.5	30.4	1.4_8

[a] Conditions: $[CL]_0 = 2.0$ mol/l, 60 °C, THF, 2 h.

[b]
$$M_n^{cal} = \frac{[CL]}{[DHPEG]} \times \text{Conversion} \times 114 + M_n^{DHPEG}. \quad (1)$$

[c]
$$M_n^{NMR} = \frac{I^h/2 \times 114}{(I^a + I^b + I^c)/4 \times 44} \times M_n^{DHPEG} + M_n^{DHPEG} = \left[\frac{I^h/2 \times 114}{(I^{a,b,i})/4 \times 44} + 1\right] \times M_n^{DHPEG}. \quad (2)$$

[d] From SEC analysis in THF (1.0 ml/min) at 25 °C with RI detector.

of CL to obtain poly(CL-*b*-PEG-*b*-CL) triblock copolymers as Scheme 1 shows.

A series of poly(CL-*b*-PEG-*b*-CL) triblock copolymers with different segment molecular weights were synthesized by adjusting the feeding molar ratio of CL to DHPEGs as shown in Table 1. The central block came from the DHPEG served as a macro-initiator while the other two from the ring-opening polymerization of ε-caprolactone. The neighboring blocks were connected through an ester linkage. ^1H NMR and ^{13}C NMR spectra of PEG_{200}–$(PCL_{2300})_2$ (Fig. 1) reveals the triblock architecture of the polymer. The characteristic signals around 4.2 ppm in ^1H NMR spectrum and

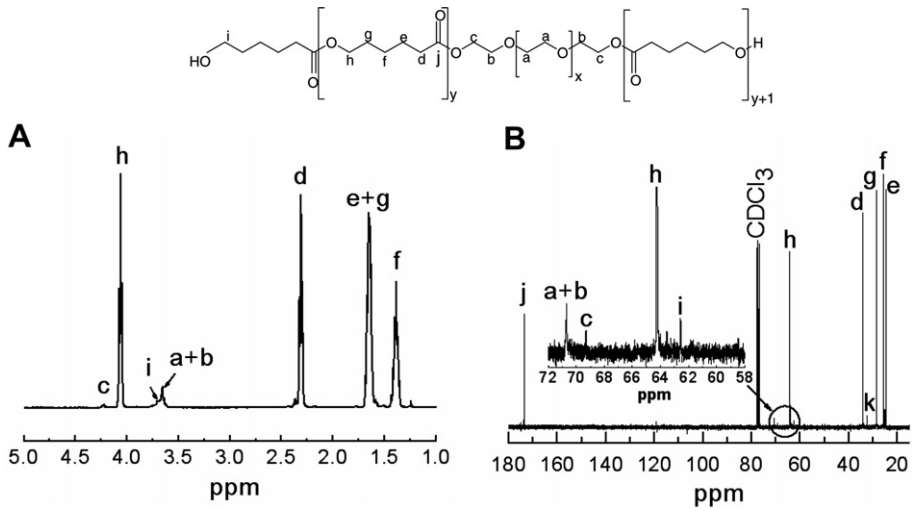

Fig. 1. ^{1}H NMR (A) and ^{13}C NMR (B) spectrum of PEG_{200}–$(PCL_{2300})_2$ in $CDCl_3$.

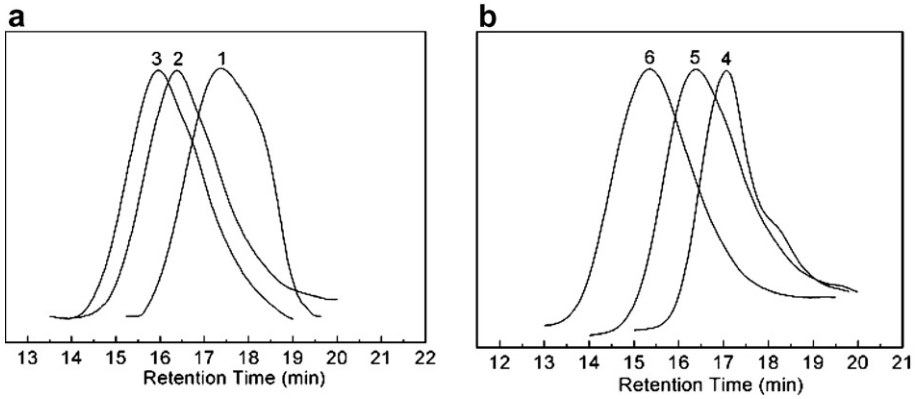

Fig. 2. SEC patterns of a: 1. PEG_{4000}–$(PCL_{3200})_2$, 2. PEG_{4000}–$(PCL_{8400})_2$ and 3. PEG_{4000}–$(PCL_{13,600})_2$; b: 4. $PEG_{10,000}$–$(PCL_{3300})_2$, 5. $PEG_{10,000}$–$(PCL_{8600})_2$ and 6. $PEG_{10,000}$–$(PCL_{14,300})_2$.

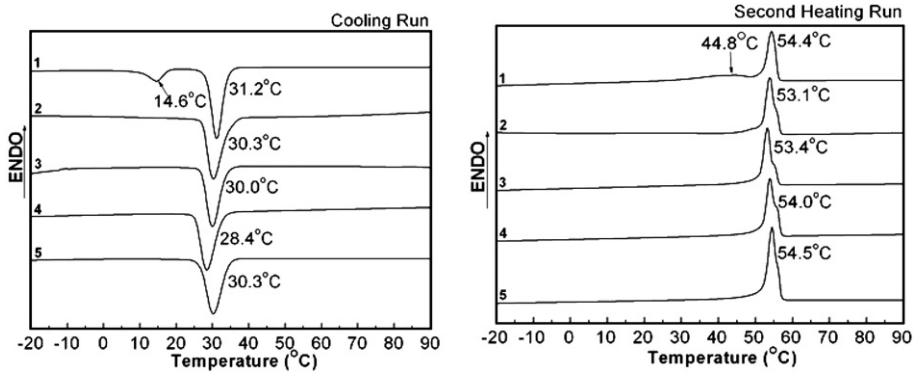

Fig. 3. DSC curves of: 1. $PEG_{10,000}$–$(PCL_{14,300})_2$; 2. PEG_{4000}–$(PCL_{13,600})_2$; 3. PEG_{2000}–$(PCL_{14,300})_2$; 4. PEG_{1000}–$(PCL_{13,800})_2$; 5. PEG_{200}–$(PCL_{14,300})_2$ with cooling and heating rate of 10 °C/min.

Table 2
Thermal properties of poly(CL-*b*-PEG-*b*-CL) triblock copolymers having similar length of PCL block and different length of PEG block

Copolymer	[a]T_c^{PEG} (°C)	[b]T_c^{PCL} (°C)	[c]ΔH_c^{PCL} (J/g)	[a]T_m^{PEG} (°C)	[b]T_m^{PCL} (°C)	[c]ΔH_m^{PCL} (J/g)
PEG_{200}–$(PCL_{14,300})_2$	–	30.3	−70.7	–	54.5	69.7
PEG_{1000}–$(PCL_{13,800})_2$	–	28.4	−70.0	–	54.0	69.2
PEG_{2000}–$(PCL_{14,300})_2$	–	30.0	−70.0	–	53.4	68.6
PEG_{4000}–$(PCL_{13,600})_2$	–	29.9	−68.9	–	53.1	70.3
$PEG_{10,000}$–$(PCL_{14,300})_2$	14.6	31.2	−70.8	40.9	54.4	–

[a] Crystallization and melting temperatures of PEG block.
[b] Crystallization and melting temperatures of PCL block.
[c] Endothermic and exothermic enthalpy of PCL block, calibrated by the wt.% of PCL block in the copolymer from ^{1}H NMR data.

69.3 ppm in ^{13}C NMR spectrum due to the proton and ^{13}C of the last –CH_2– group in DHPEG segment next to the –COO– group of PCL block were clearly observed. The molecular weights of the triblock products were determined by ^{1}H NMR end group analysis following Eq. (2), which were very close to the values calculated by the apparent conversions and the feeding molar ratios of CL to DHPEG (Eq. (1)) indicating that the exchange reaction of yttrium alkoxide and hydroxyl end group is essential for controlling products' molecular weights [20].

Fig. 2 shows the SEC patterns of poly(CL-*b*-PEG-*b*-CL) triblock copolymers with $DHPEG_{4000}$ and $DHPEG_{10,000}$ as macro-initiators, respectively. With the same macro-initiator, the molecular weight increased with the increasing molar ratio of CL to DHPEG and the molecular weight distribution remain single peak suggesting only one kind of active center in the polymerization system.

3.2. Thermal and crystallization properties

The DSC curves of PEG_{200}–$(PCL_{14,300})_2$, PEG_{1000}–$(PCL_{13,800})_2$, PEG_{2000}–$(PCL_{14,300})_2$, PEG_{4000}–$(PCL_{13,600})_2$, and $PEG_{10,000}$–$(PCL_{14,300})_2$ with similar molecular weight of PCL blocks ($M_n \approx 14{,}000$) and different molecular weights of PEG blocks (varying from 200 to 10,000) are displayed in Fig. 3. All samples were firstly heated to 100 °C and held for 2 min to erase the thermal history, then cooled to −30 °C at a cooling rate of 10 °C/min, and finally heated to 100 °C again by a rate of 10 °C/min. There are only one exothermic peak and one endothermic peak due to the PCL block in all triblock copolymers observed in the curves except $PEG_{10,000}$–$(PCL_{14,300})_2$ with another exothermic peak at 14.6 °C and endothermic peak at 44.8 °C due to the $PEG_{10,000}$ block, which illustrates that when the PCL blocks in the copolymers are rather long ($M_n \approx 14{,}000$), the PEG block could crystallize only when they are long enough such as $PEG_{10,000}$(26 wt.%). The data of thermal behaviors of the copolymers are shown in Table 2, from which it could be summarized that the lengths of PEG blocks have almost no influence on the T_cs, T_ms, ΔH_cs and ΔH_ms of the PCL blocks. However, the

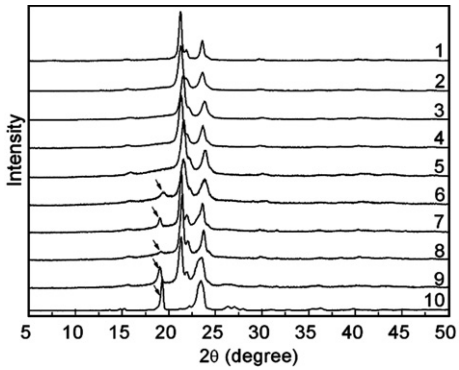

Fig. 4. WAXD patterns of 1. $PCL_{30,000}$; 2. PEG_{200}–$(PCL_{14,300})_2$; 3. PEG_{1000}–$(PCL_{13,800})_2$; 4. PEG_{2000}–$(PCL_{14,300})_2$; 5. PEG_{4000}–$(PCL_{13,600})_2$; 6. $PEG_{10,000}$–$(PCL_{14,300})_2$; 7. PEG_{2000}–$(PCL_{1800})_2$; 8. PEG_{2000}–$(PCL_{3600})_2$; 9. PEG_{4000}–$(PCL_{3200})_2$; 10. $PEG_{10,000}$.

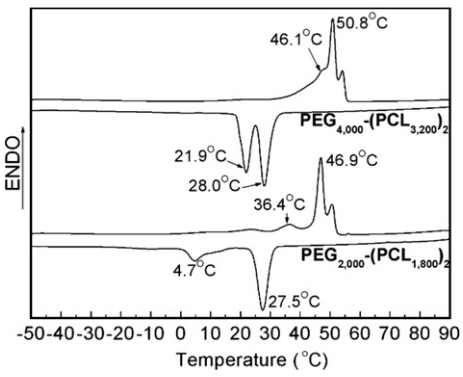

Fig. 5. DSC curves of PEG_{2000}–$(PCL_{1800})_2$ and PEG_{4000}–$(PCL_{3200})_2$ with cooling and heating rate of 10 °C/min.

PCL blocks influence the crystallization of PEG blocks evidently as discussed above.

The WAXD patterns of PEG_{200}–$(PCL_{14,300})_2$, PEG_{1000}–$(PCL_{13,800})_2$, PEG_{2000}–$(PCL_{14,300})_2$, PEG_{4000}–$(PCL_{13,600})_2$ and $PEG_{10,000}$–$(PCL_{14,300})_2$were shown in Fig. 4(2–6) with that of $PCL_{30,000}$ (1) and $DHPEG_{10,000}$ (10) as comparisons. When the copolymer has long PCL blocks ($M_n \approx 14{,}000$) and short PEG block ($M_n < 10{,}000$), the PEG block cannot crystallize and form separate crystal phase because no characteristic signal at around $2\theta = 19°$ due to the crystallization of PEG block was detected. The results match DSC analyses quite well.

Fig. 5 displays the DSC analysis of PEG_{2000}-$(PCL_{1800})_2$ and PEG_{4000}–$(PCL_{3200})_2$, in which two exothermic peaks and two endothermic peaks due to the PCL block and PEG block were detected clearly. As shown in Fig. 4(7–9), both the PCL and PEG blocks in PEG_{2000}–$(PCL_{1800})_2$, PEG_{2000}–$(PCL_{3600})_2$ and PEG_{4000}–$(PCL_{3200})_2$ can crystallize

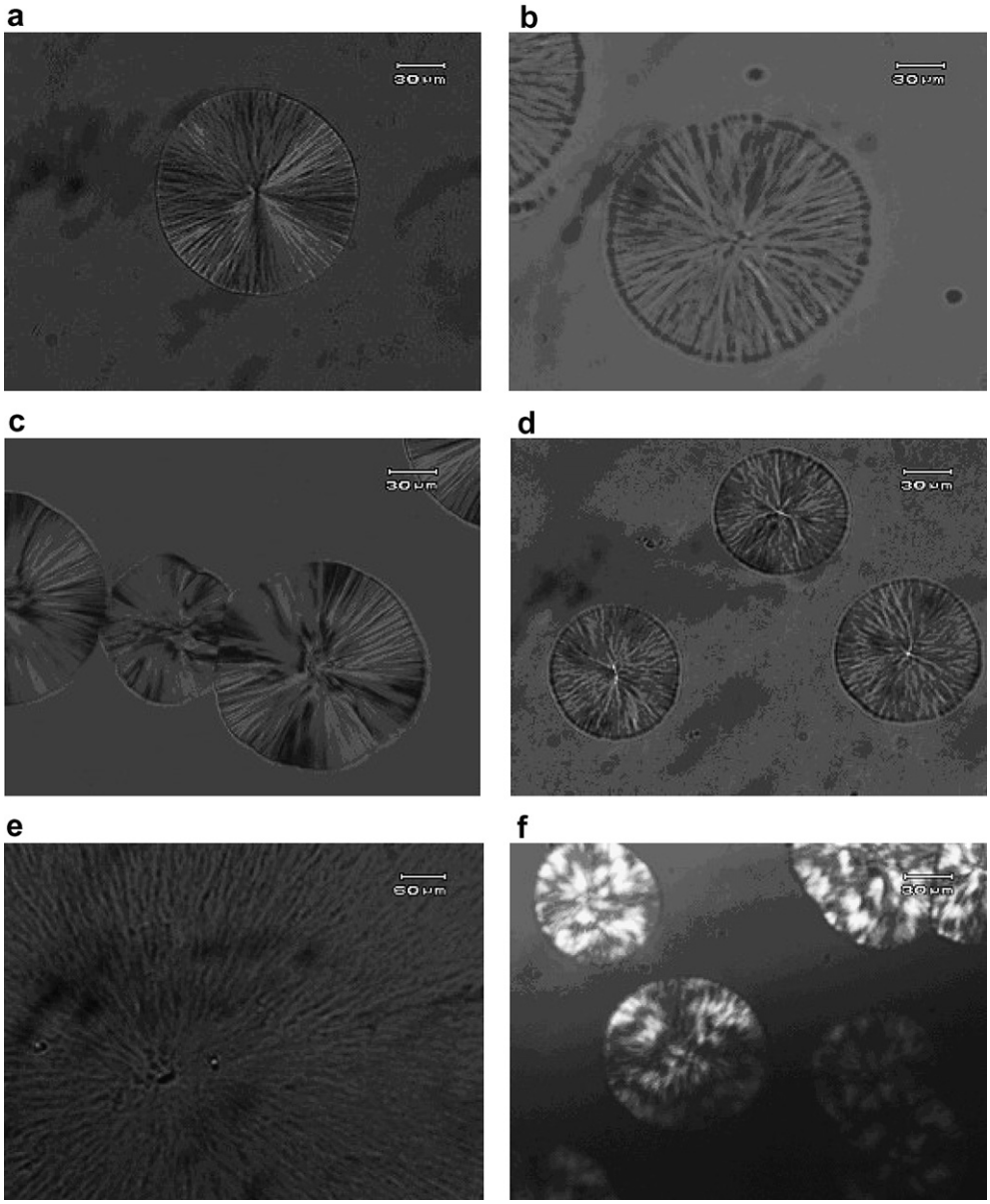

Fig. 6. POM micrographs of spherulites of (a) PEG_{1000}–$(PCL_{13,800})_2$; (b) PEG_{2000}–$(PCL_{14,300})_2$; (c) PEG_{4000}–$(PCL_{13,600})_2$; (d) $PEG_{10,000}$–$(PCL_{14,300})_2$; (e) $DHPEG_{10,000}$ and (f) $PCL_{30,000}$, crystallized at 45 °C for 15 min.

and form separate crystal phases. So it could be concluded that when the lengths of PCL blocks are short, even the short PEG block ($M_n = 2000$) can crystallize.

3.3. Isothermal crystallization behaviors on POM

Fig. 6 shows the POM micrograph of the triblock copolymers with various PEG block lengths and fixed PCL block length ($M_n \approx 14{,}000$) isothermal crystallized at 45 °C for 15 min, as well as those of pure $DHPEG_{10,000}$ and $PCL_{30,000}$ as comparisons. The spherulite of $DHPEG_{10,000}$ (Fig. 6e) is larger and grows faster than the spherulite of $PCL_{30,000}$ (Fig. 6f). However, spherulite morphology and crystallization rate of the triblock copolymers (Fig. 6a–d) are similar to homo-polymer of PCL rather than homo-polymer of DHPEG. The crystallization ability of PEG block was restrained by the long PCL block beside them, and the PCL block can crystallize alone excluding PEG block. This result is in agreement with the DSC and WAXD analyses.

The POM micrograph of copolymers with short PCL blocks such as PEG_{2000}–$(PCL_{1800})_2$, PEG_{2000}–$(PCL_{3600})_2$, PEG_{4000}–$(PCL_{2300})_2$ and PEG_{4000}–$(PCL_{3200})_2$ show poor spherulite morphologies (Fig. 7), which indicates that both PCL block and PEG block can crystallize, but the mutual influence between them obviously led to imperfect spherulite morphologies.

Fig. 8 shows the real-time changes of the crystallization of $PEG_{10,000}$–$(PCL_{8600})_2$. An interesting morphology of the concentric spherulites was observed in the POM micrograph. At the beginning, the spherulite blocks generated and grew slowly (Fig. 8a–c). About 16 min later, a quite different outer ring began to grow quickly, resulting in the formation of a concentric (Fig. 8d–f). In the concentric spherulites, the morphology and growing rate of the central ring is quite different from that of the outer one; the former is similar to that of the PCL block (Fig. 6f), while that of the latter to PEG (Fig. 6e). According to the morphologies and crystallization rates, the central and outer spherulites

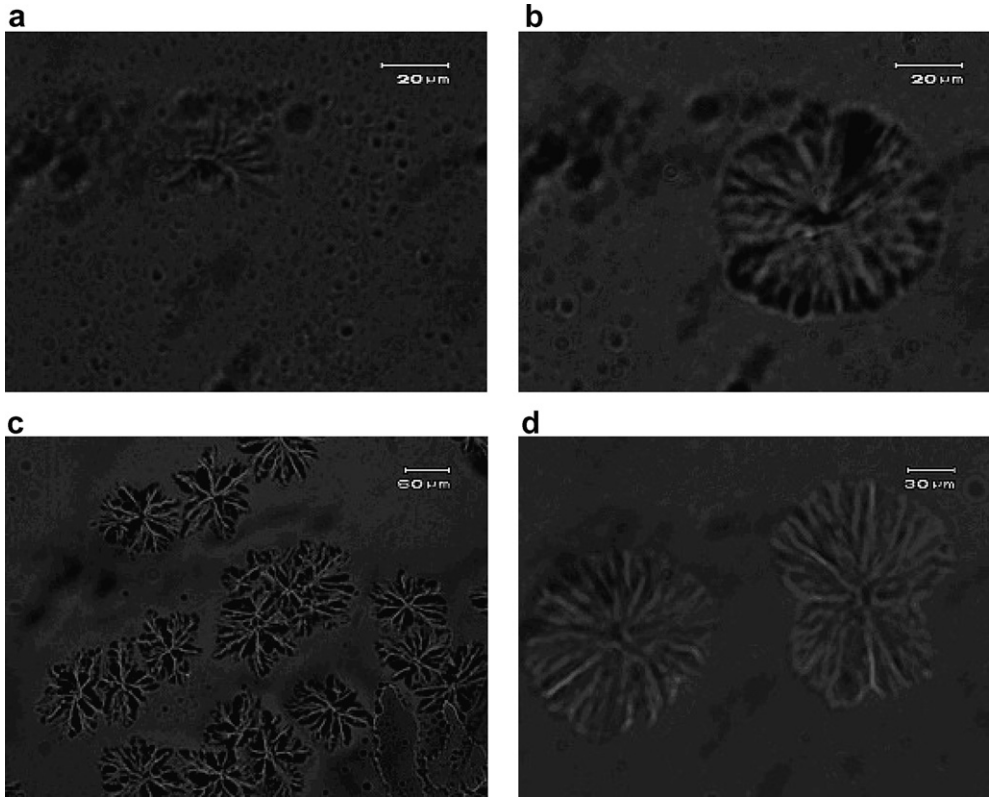

Fig. 7. POM micrographs of spherulites of triblock copolymers with short PCL blocks: (a) PEG_{2000}–$(PCL_{1800})_2$; (b) PEG_{2000}–$(PCL_{3600})_2$; (c) PEG_{4000}–$(PCL_{2300})_2$ and (d) PEG_{4000}–$(PCL_{3200})_2$, crystallized at 45 °C for 15 min.

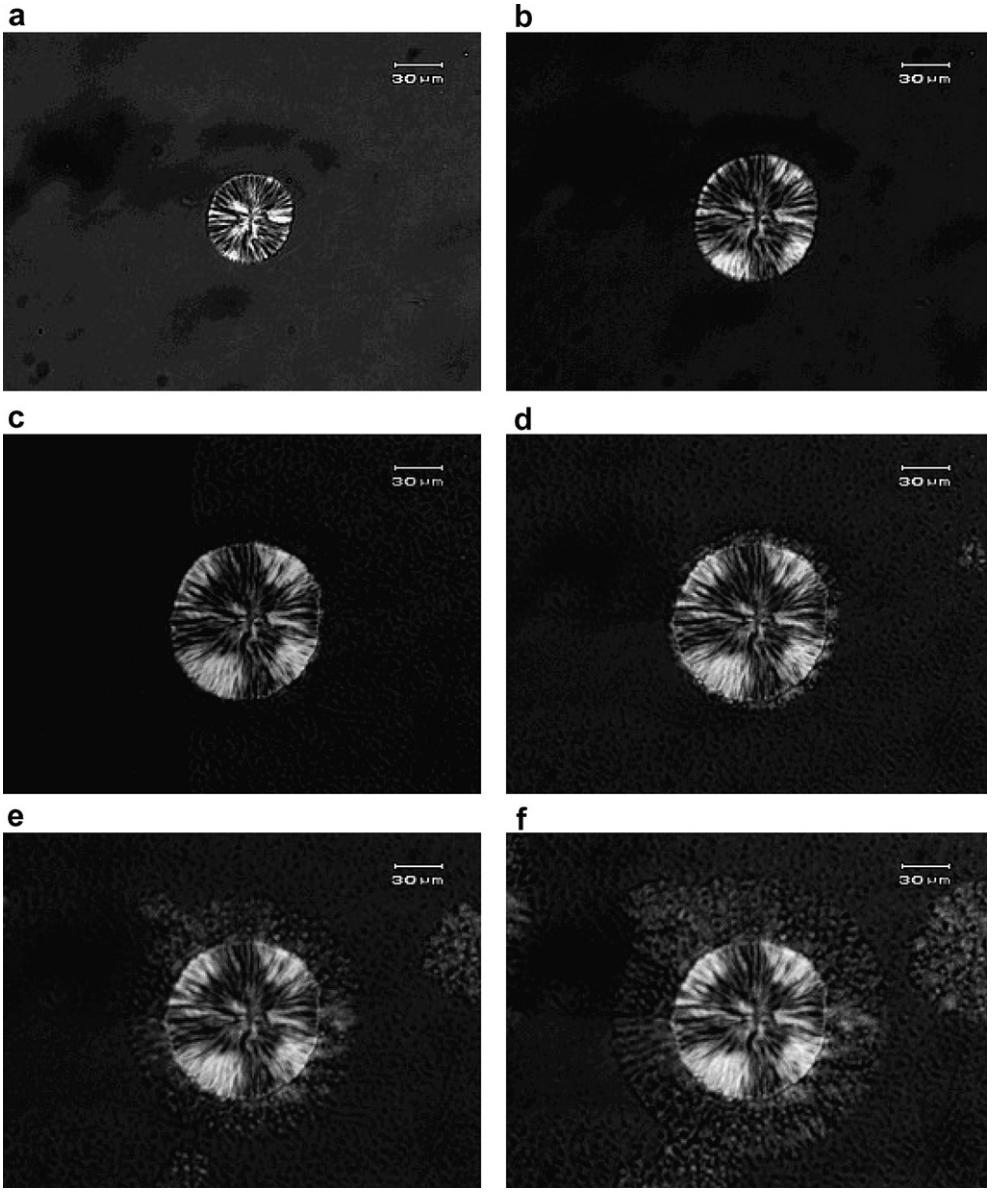

Fig. 8. Growth process of concentric spherulites of $PEG_{10,000}$–$(PCL_{8600})_2$, crystallized at 45 °C.

can be assigned to the PCL and PEG components, respectively. When the lengths of the PCL and PEG blocks are close and long enough, the spherulites of the PCL block occurs first because of its higher T_c and grew exclusively, and then the spherulite of PEG block developed from the growth front of the PCL spherulite.

4. Conclusions

In this article, well-defined amphiphilic poly(CL-*b*-PEG-*b*-CL) triblock copolymers were synthesized successfully by double-hydroxyl capped poly(ethylene glycol) (DHPEG) as macro-initiator in the presence of yttrium tris(2,6-di-tert-butyl-4-methylphenolate) [$Y(DBMP)_3$]. The triblock architecture was characterized by NMR spectra thoroughly. As the results of DSC, WAXD and POM analyses, the crystallization behaviors of the copolymers are greatly influenced by the length of each block. When the PCL blocks are long, they can crystallize alone excluding PEG block, and the short PEG block cannot crystallize. While the PCL blocks are short, both PCL and PEG blocks can crystallize, but the

mutual influence between them leads to poor morphology on POM micrograph. And as the lengths of the PCL and PEG blocks are close and long enough, the sequent crystallization of PCL and PEG blocks make an interesting morphology of concentric spherulites on POM micrograph.

Acknowledgements

The authors gratefully acknowledge financial supports from the National Natural Science Foundation of China (Key program 20434020), special fund for the Major State Basic Research Project (2005CB623802), China Postdoctor Science Foundation (20060390334) and the Committee of Science and Technology of Zhejiang Province (Y404041).

References

[1] Liu TB, Burger V, Chu B. Nanofabrication in polymer matrices. Prog Polym Sci 2003;28(1):5–26.
[2] Aseyev VO, Tenhu H, Winnik FM. Temperature dependence of the colloidal stability of neutral amphiphilic polymers in water. Adv Polym Sci 2006;196:1–85.
[3] Wang F, Bronich TK, Kabanov AV, Rauh RD, Roovers J. Synthesis and evaluation of a star amphiphilic block copolymer from poly(epsilon-caprolactone) and poly(ethylene glycol) as a potential drug delivery carrier. Bioconjugate Chem 2005;16(2):397–405.
[4] Kwon GS, Forrest ML. Amphiphilic block copolymer micelles for nanoscale drug delivery. Drug Dev Res 2006;67(1):15–22.
[5] Webber GB, Wanless EJ, Armes SP, Baines FL, Biggs S. Adsorption of amphiphilic diblock copolymer micelles at the mica/solution interface. Langmuir 2001;17(18):5551–61.
[6] Albertsson AC, Varma IK. Recent developments in ring opening polymerization of lactones for biomedical applications. Biomacromolecules 2003;4(6):1466–86.
[7] Andersson L, Davies J, Duncan R. Poly(ethylene glycol)–poly(ester-carbonate) block copolymers carrying PEG-peptidyl-doxorubicin pendant side chains: Synthesis and evaluation as anticancer conjugates. Biomacromolecules 2005; 6(2):914–26.
[8] Tian HY, Deng C, Lin H, Sun JR, Deng MX, Chen XS, et al. Biodegradable cationic PEG-PEI-PBLG hyperbranched block copolymer: synthesis and micelle characterization. Biomaterials 2005;26(20):4209–17.
[9] Zhou SB, Deng XM, Yang H. Biodegradable poly(epsilon-caprolactone)-poly(ethylene glycol) block copolymers: characterization and their use as drug carriers for a controlled delivery system. Biomaterials 2003;24(20):3563–70.
[10] Guan HL, Xie ZG, Zhang PB, Wang X, Chen XS, Wang XH, et al. Synthesis and characterization of novel biodegradable block copolymer poly(ethylene glycol)-block-poly (L-lactide-co-2-methyl-2-carboxyl-propylene carbonate). J Polym Sci Part A: Polym Chem 2005;43(20):4771–80.
[11] Piao LH, Dai ZL, Deng XM, Chen XS, Jing XB. Synthesis and characterization of PCL/PEG/PCL triblock copolymers by using calcium catalyst. Polymer 2003;44(7):2025–31.
[12] Yang J, Jia L, Yin LZ, Yu JY, Shi Z, Fang Q, et al. A novel approach to biodegradable block copolymers of epsilon-caprolactone and delta-valerolactone catalyzed by new aluminum metal complexes. Macromol Biosci 2004;4(12): 1092–104.
[13] Gan ZH, Zhang J, Jiang BZ. Poly(epsilon-capralactone)/poly(ethylene oxide) diblock copolymer. 2. Nonisothermal crystallization and melting behavior. J Appl Polym Sci 1997;63(13):1793–804.
[14] He CL, Sun JR, Zhao T, Hong ZK, Zhuang XL, Chen XS, et al. Formation of a unique crystal morphology for the poly(ethylene glycol)–poly(epsilon-caprolactone) diblock copolymer. Biomacromolecules 2006;7(1):252–8.
[15] He CL, Sun JR, Deng C, Zhao T, Deng XM, Chen XS, et al. Study of the synthesis, crystallization, and morphology of poly(ethylene glycol)-poly(is an element of-caprolactone) diblock copolymers. Biomacromolecules 2004;5(5): 2042–7.
[16] Ling J, Shen ZQ. Lanthanum tris(2,6-di-tert-butyl-4-methylphenolate) as a novel, versatile initiator for homo- and copolymerization of cyclic carbonates and lactones. Macromol Chem Phys 2002;203(4):735–8.
[17] Ling J, Zhu WP, Shen ZQ. Controlling ring-opening copolymerization of epsilon-caprolactone with trimethylene carbonate by scandium tris(2,6-di-tert-butyl-4-methylphenolate). Macromolecules 2004;37(3):758–63.
[18] Zhu WP, Ling J, Shen ZQ. Homopolymerization of epsilon-caprolactone initiated by a scandium aryloxide. Polym Bull 2004;52(3-4):185–9.
[19] Peng F, Ling J, Shen ZQ, Zhu WW. Correlation between phenol structure and catalytic activity of samarium(III) phenolates in polymerization of epsilon-caprolactone – Part 2. Tertbutyl's electronic and steric effects. J Mol Catal A-Chem 2005;230(1–2):135–41.
[20] Ling J, Chen W, Shen ZQ. Synthesis and characterization of poly(DTC-b-PEG-b-DTC) triblock and poly(TMC-b-DTC-b-PEG-b-DTC-b-TMC) pentablock copolymers and kinetics of the polymerization. J Polym Sci Part A: Polym Chem 2005;43(9):1787–96.